

# The Isomorphism of $H_4$ and $E_8$

J Gregory Moxness\*  
*TheoryOfEverything.org*  
 (Dated: October 28, 2023)

This paper gives an explicit isomorphic mapping from the 240 real  $\mathbb{R}^8$  roots of the  $E_8$  Gossett  $4_{21}$  8-polytope to two golden ratio scaled copies of the 120 root  $H_4$  600-cell quaternion 4-polytope using a traceless  $8 \times 8$  rotation matrix  $\mathbb{U}$  with palindromic characteristic coefficients and a unitary form  $e^{i\mathbb{U}}$ . It also shows the inverse map from a single  $H_4$  600-cell to  $E_8$  using a  $4\text{D} \leftrightarrow 8\text{D}$  chiral left  $\leftrightarrow$  right mapping function,  $\varphi$  scaling, and  $\mathbb{U}^{-1}$ . This approach shows that there are actually four copies of each 600-cell living within  $E_8$  in the form of chiral  $H_{4L} \oplus \varphi H_{4L} \oplus H_{4R} \oplus \varphi H_{4R}$  roots. In addition, it demonstrates a quaternion Weyl orbit construction of  $H_4$ -based 4-polytopes that provides an explicit mapping between  $E_8$  and four copies of the tri-rectified Coxeter-Dynkin diagram of  $H_4$ , namely the 120-cell of order 600. Taking advantage of this property promises to open the door to as yet unexplored  $E_8$ -based Grand Unified Theories or GUTs.

PACS numbers: 02.20.-a, 02.10.Yn  
 Keywords: Coxeter groups, root systems, E8

## I. INTRODUCTION

Fig. 1 is the Petrie projection of the Gossett  $4_{21}$  8-polytope derived from the Split Real Even (SRE) form of the  $E_8$  Lie group with unimodular lattice in  $\mathbb{R}^8$ . It has 240 vertices and 6,720 edges of 8-dimensional (8D) length  $\sqrt{2}$ .  $E_8$  is the largest of the exceptional simple Lie algebras, groups, and lattices. An important and related higher dimensional structure is the  $\mathbb{R}^{24}$  ( $\mathbb{C}^{12}$ ) Leech lattice ( $\Lambda_{24} \supset E_8 \otimes E_8 \otimes E_8$ ), with its binary (ternary) Golay code construction.

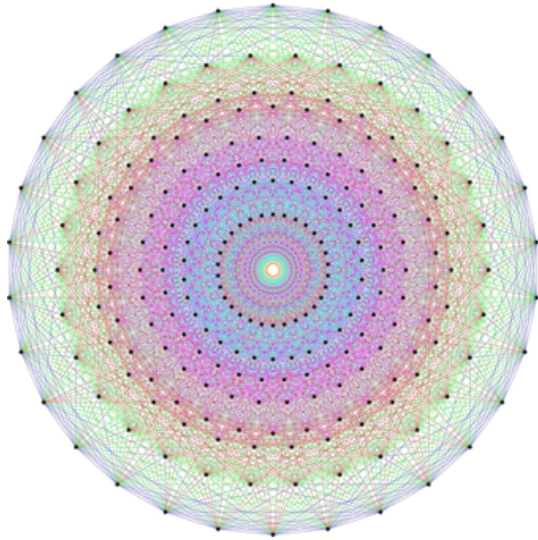


FIG. 1.  $E_8$   $4_{21}$  Petrie projection

It is widely known [1]-[14] that the  $E_8$  can be pro-

jected, mapped, or "folded" (as shown in Fig. 2) to two golden ratio ( $\varphi = \frac{1}{2}(1 + \sqrt{5}) \approx 1.618$ ) scaled copies of the 4 dimensional 120 vertex 720 edge  $H_4$  600-cell. Folding an 8D object into a 4 dimensional one can be done by projecting each vertex using its dot product with a  $4 \times 8$  matrix[11]. This produces  $H_4 \oplus \varphi H_4$ , where  $H_4$  is the binary icosahedral group  $2I$  of order 120, a subgroup of  $\text{Spin}(3)$ . It covers  $H_3$  as the full icosahedral group  $I_h$  of order 120, a subgroup of  $\text{SO}(3)$ . The binary icosahedral group can be considered as the double cover of the alternating group alternating group  $A_5$ .

Despite others'[2][9] recent attempts, the inverse morphism or "unfolding" from  $H_4$  to  $E_8$  is less trivial given that the matrix is not square and lacks an inverse. Yet, a real ( $\mathbb{R}$ ) symmetric volume preserving  $\text{Det}(\mathbb{U})=1$  rotation matrix(1) was derived in 2012 and documented[11][12][13]. The quadrant structure of  $\mathbb{U}$  rotates  $E_8$  into four 4D copies of  $H_4$  600-cells, with the original two (L)eft and (R)ight side unit scaled 4D copies related to the two L/R  $\varphi$  scaled copies which we now identify as  $H_4(L \oplus R \oplus 1 \oplus \varphi)$ . This traceless form of  $\mathbb{U}$  has palindromic characteristic coefficients and provides for an explicit isomorphic mapping of  $E_8 \leftrightarrow H_4(L \oplus R \oplus 1 \oplus \varphi)$ . This involves using a bidirectional L  $\leftrightarrow$  R mapping function (mapLR) and  $\mathbb{U}^{-1}$ (2). The process is described and visualized in Section II.

$$\mathbb{U} = \begin{pmatrix} 1 - \varphi & 0 & 0 & 0 & 0 & 0 & 0 & 0 & -\varphi^2 \\ 0 & -1 & \varphi & 0 & 0 & \varphi & 1 & 0 & 0 \\ 0 & \varphi & 0 & 1 & -1 & 0 & \varphi & 0 & 0 \\ 0 & 0 & -1 & \varphi & \varphi & 1 & 0 & 0 & 0 \\ 0 & 0 & 1 & \varphi & \varphi & -1 & 0 & 0 & 0 \\ 0 & \varphi & 0 & 1 & -1 & 0 & \varphi & 0 & 0 \\ 0 & 1 & \varphi & 0 & 0 & \varphi & -1 & 0 & 0 \\ -\varphi^2 & 0 & 0 & 0 & 0 & 0 & 0 & 0 & 1 - \varphi \end{pmatrix} / (2\sqrt{\varphi}) \tag{1}$$

\* <https://www.TheoryOfEverything.org/theToE>;  
 mailto:jgmoxness@TheoryOfEverything.org

$$U^{-1} = \frac{1}{(2\sqrt{\varphi})} \begin{pmatrix} \varphi - 1 & 0 & 0 & 0 & 0 & 0 & 0 & 0 & -\varphi^2 \\ 0 & -\varphi & 1 & 0 & 0 & 1 & \varphi & 0 & 0 \\ 0 & 1 & 0 & \varphi & -\varphi & 0 & 1 & 0 & 0 \\ 0 & 0 & -\varphi & 1 & 1 & \varphi & 0 & 0 & 0 \\ 0 & 0 & \varphi & 1 & 1 & -\varphi & 0 & 0 & 0 \\ 0 & 1 & 0 & \varphi & -\varphi & 0 & 1 & 0 & 0 \\ 0 & \varphi & 1 & 0 & 0 & 1 & -\varphi & 0 & 0 \\ -\varphi^2 & 0 & 0 & 0 & 0 & 0 & 0 & 0 & \varphi - 1 \end{pmatrix} \quad (2)$$

### A. Generating Polytopes

The quaternion ( $\mathbb{H}$ ) Weyl group orbit  $O(\Lambda) = W(H_4) = I$  of order 120 is constructed from the parent orbit (1000) of the Coxeter-Dynkin diagram for  $H_4$  shown in Fig. 2b. This results in the 600-cell 4-polytope of order 120 labeled here and in [3] as I. In addition,  $U$  provides for a direct mapping from  $E_8$  to four  $L \oplus R \oplus 1 \oplus \varphi$  copies of the tri-rectified parent of  $H_4$  (i.e. the filled node 1 is shifted right 3 times giving 0001), which is the 120-cell of order 600 labeled here and in [3] as J. Both of these 4-polytopes are shown in Appendix A Figs. 14-16. The detail of the quaternion Weyl orbit construction is described in Section III.

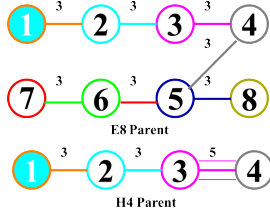


FIG. 2. a)  $E_8$  Dynkin diagram in folding orientation  
b) The associated Coxeter-Dynkin diagram of  $H_4$

In addition to the 240 root  $4_{21}$   $E_8$  8-polytope identified by its Coxeter-Dynkin diagram in Fig. 3a, there are  $2^8$  possible orbits using only 0's  $\leftrightarrow$  1's, empty  $\leftrightarrow$  filled, or ringed nodes of the  $E_8$  Coxeter-Dynkin diagram, including the snub (00000000) orbit. Several other orbit permutations are commonly represented visually using the Petrie projection basis. They are the 2,160 root  $2_{41}$  and 17,280 root  $1_{42}$  8-polytopes, which are constructed by generating the resulting roots by moving the filled (or ringed) node to each of the two other ends of the Dynkin diagram, as shown in Figs. 3b and 3c respectively.

### B. 8D Platonic Rotation

Interestingly from [13],  $U$  can be generated using a combination of the unimodular matrices commonly used for Quantum Computing (QC) qubit logic, namely those of the 2 qubit CNOT (3) and SWAP (4) gates. Taking these patterns, combined with the recursive functions

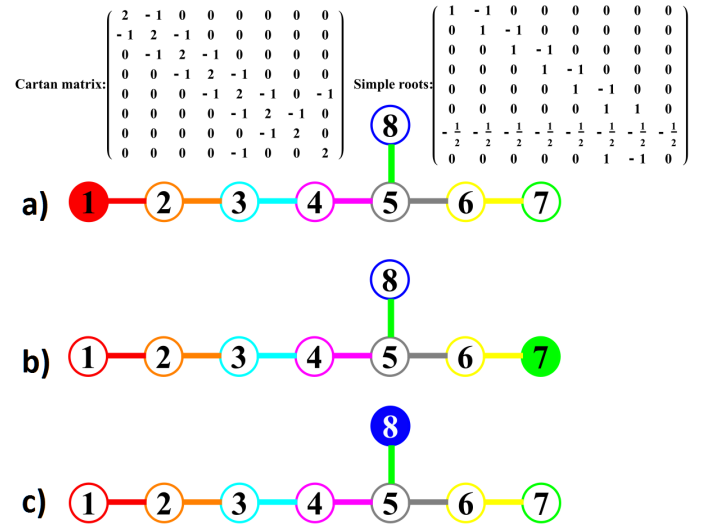


FIG. 3.  $E_8$  Dynkin diagrams a)  $4_{21}$ , b)  $2_{41}$ , c)  $1_{42}$   
Also shown are the Cartan and simple root matrices which correspond to the common Coxeter-Dynkin representation of the diagrams.

that build  $\varphi$  from the Fibonacci sequence, it is straightforward to derive  $U$  from scaled QC logic gates.[14]

$$\text{CNOT} = \begin{pmatrix} 1 & 0 & 0 & 0 \\ 0 & 1 & 0 & 0 \\ 0 & 0 & 0 & 1 \\ 0 & 0 & 1 & 0 \end{pmatrix} \quad (3)$$

$$\text{SWAP} = \begin{pmatrix} 1 & 0 & 0 & 0 \\ 0 & 0 & 1 & 0 \\ 0 & 1 & 0 & 0 \\ 0 & 0 & 0 & 1 \end{pmatrix} \quad (4)$$

### C. 2D and 3D Projection

Projection of  $E_8$  to 2D (or 3D) requires 2 (or 3) basis vectors  $\{X, Y, Z\}$ . For the Petrie projection shown in Fig. 1, we start with the basis vectors in (5), which are simply the two 2D Petrie projection basis vectors of the 600-cell (a.k.a. the Van Oss projection), with an optional 3rd (z) basis vector added for an interesting 3D projection[11].

$$\begin{aligned} x &= \{ 0, \varphi 2 \sin \frac{2\pi}{15}, 2 \sin \frac{2\pi}{15}, 0, 0, 0, 0, 0 \} \\ y &= \{ -\varphi 2 \sin \frac{2\pi}{30}, 0, 0, 1, 0, 0, 0, 0 \} \\ z &= \{ 1, 0, 0, \varphi 2 \sin \frac{2\pi}{30}, 0, 0, 0, 0 \} \end{aligned} \quad (5)$$

$\{X, Y, Z\} = U \cdot \{x, y, z\}$  as shown in (6).

$$\begin{aligned} X &= \{ 0 \quad .252 \quad .427 \quad -.319 \quad .319 \quad .427 \quad .781 \quad 0 \} \\ Y &= \{ .821 \quad 0 \quad -.393 \quad .636 \quad .636 \quad .393 \quad 0 \quad .348 \} \\ Z &= \{ -.242 \quad 0 \quad -.132 \quad .215 \quad .215 \quad .132 \quad 0 \quad -1.03 \} \end{aligned} \quad (6)$$

### D. 3D Platonic Solid Projection

This basis is derived from the icosahedral symmetry of  $H_3$ -based Platonic solid. The twelve vertices of the icosahedron can be decomposed into three mutually-perpendicular golden rectangles (as shown in Fig. 4), whose boundaries are linked in the pattern of the Borromean rings. Rows (or columns) 2-4 (or 5-8) of  $\mathbb{U}$  contain 6 of the 12 vertices of this icosahedron, including 2 at the origin with the other 6 of 12 icosahedron vertices being the antipodal reflection of these through the origin. These 2 (or 3) rows can then be used as a kind of “Platonic solid projection prism” to form the 2 (or 3) 8D basis vectors used in the 2D (or 3D) projection of  $4_{21}$ ,  $2_{41}$ , and  $1_{42}$ .

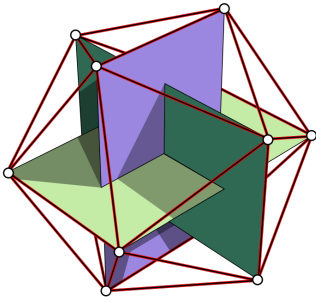
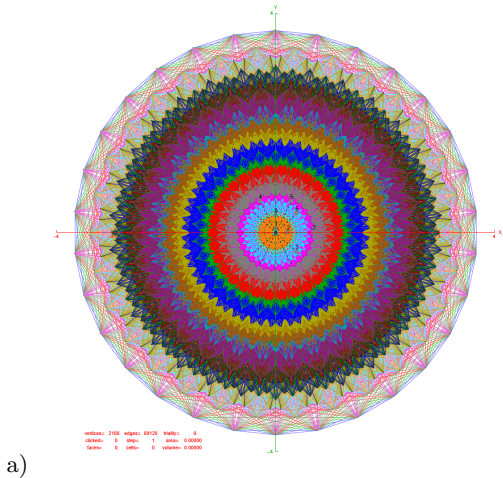
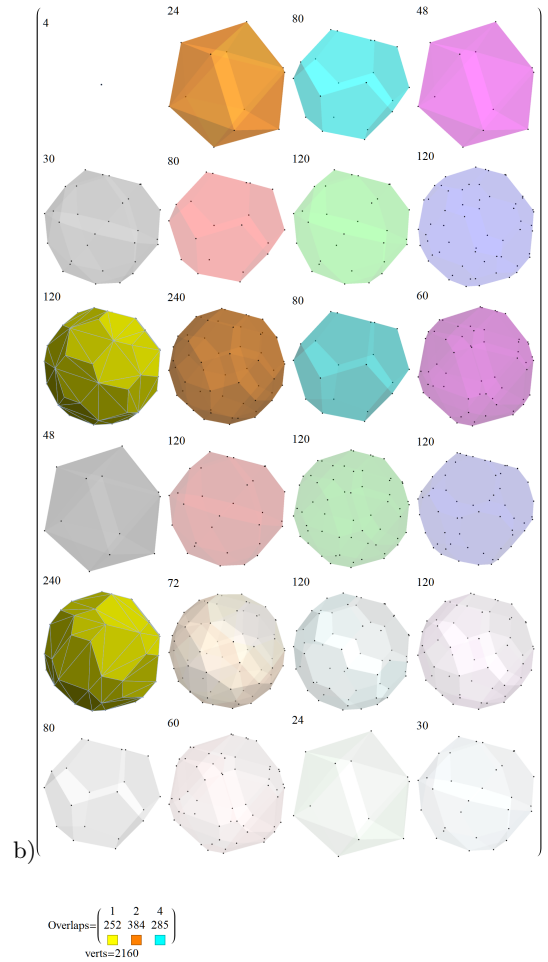


FIG. 4. The icosahedron formed from 3 mutually-perpendicular golden rectangles

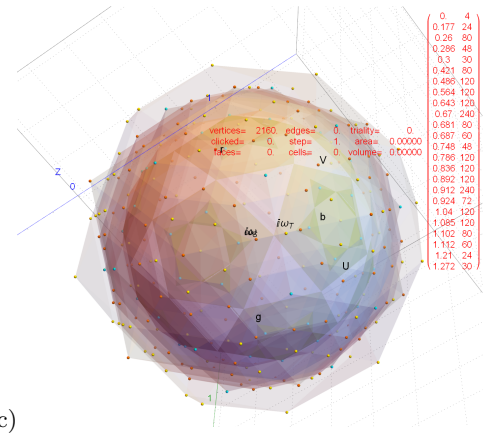
Orthogonal projection to 3D after  $\mathbb{U}$  folding (i.e. selecting one of 56 unique subsets of 3 (of 8) dimensions, here we use  $\{1, 2, 3\}$ ) manifests a large number of concentric hulls with Platonic and Archimedean solid related structures. The eight projected 3D hulls of  $4_{21}$  include two  $\varphi$  scaled sets of four hulls from two 600-cells ( $H_4 \oplus \varphi H_4$ ) as shown in Appendix A Fig. 14.  $2_{41}$  and  $1_{42}$  projections of  $E_8$  are shown in Figs. 5-6.



a)



b)



c)

FIG. 5.  $2_{41}$  projections of its 2,160 vertices  
a) 2D to the  $E_8$  Petrie projection using basis vectors X and Y from (6) with 8-polytope radius  $2\sqrt{2}$  and 69,120 edges of length  $\sqrt{2}$   
b) 3D projections with vertices sorted and tallied by their 3D norm generating the increasingly transparent hulls for each set of tallied norms. Notice the last two outer hulls are a combination of two overlapped Icosahedrons (24) and a Icosidodecahedron (30).  
c) Combined 3D hulls with the overlapping vertices color coded by overlap count. Also shown is a list (in red) the normed hull distance and the number of vertices in the group.

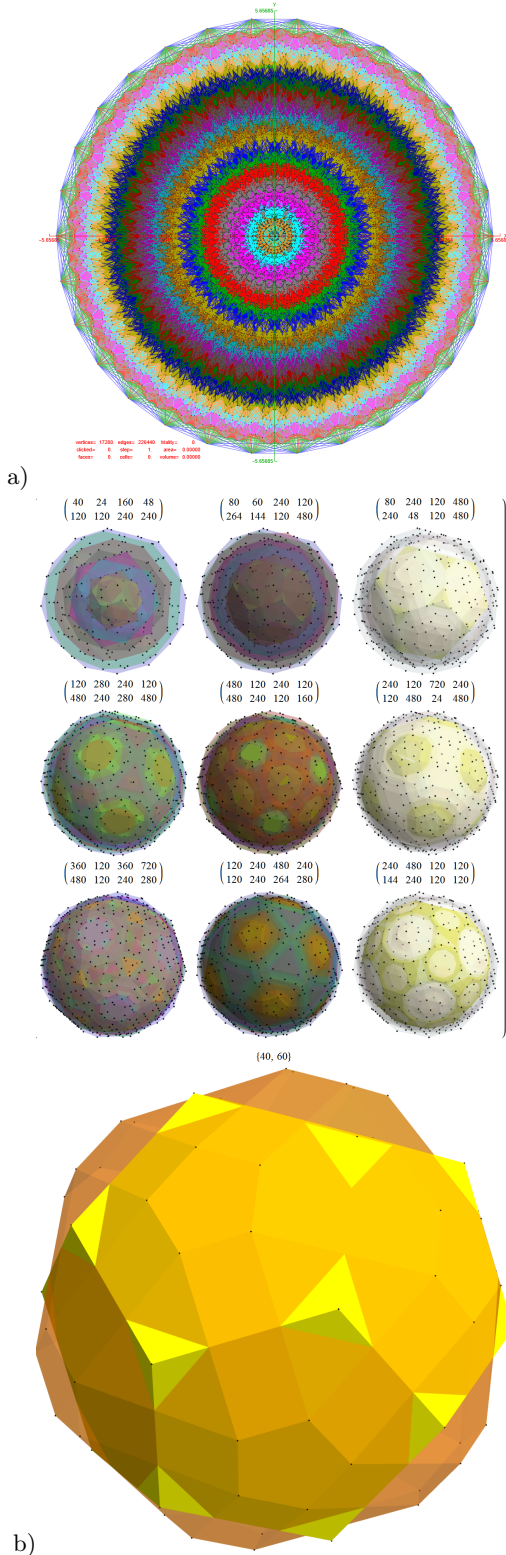


FIG. 6. 142 projections of its 17,280 vertices  
a) 2D to the  $E_8$  Petrie projection using basis vectors X and Y from (6) with 8-polytope radius  $4\sqrt{2}$  and 483,840 edges of length  $\sqrt{2}$  (with 53% of inner edges culled for display clarity)  
b) 3D projections with vertices sorted and tallied by their 3D norm generating the increasingly transparent hulls for each set of tallied norms. Notice the last two outer hulls are a combination of two overlapped Dodecahedrons (40) and a irregular Rhombicosidodecahedron (60).

## II. THE PALINDROMIC UNITARY MATRIX

The particular maximal embedding of  $E_8$  at height 248 that we are interested in for this work is shown in Appendix C Fig. 19 as the special orthogonal group of  $SO(16)=D_8$  at height  $(120=112+4+4)+128'$ , where 112 is interpreted as the subgroup embeddings of  $SO(8)\otimes SO(8)=D_4\otimes D_4$  and  $128'$  is interpreted as symplectic subgroup embeddings of  $C_8$  where  $Sp(8)\otimes Sp(8)=C_4\otimes C_4$  at height  $136=128+4+4$ . These selected embeddings correspond to the 112 integer  $D_8$  vertices and the 128 half-integer  $BC_8$  vertices given by SRE  $E_8$ , in addition to the  $8\oplus\bar{8}$  generator roots for a total of  $2^8$ . This is in 1::1 correspondence with the canonical root vertex ordering from the 9th row of the palindromic Pascal triangle  $\{1, 8, 28, 56, 35\bar{3}\bar{5}, \bar{5}\bar{6}, \bar{2}\bar{8}, \bar{8}, \bar{1}\}$ , where each entry in the list gives the number of vertices that alternate between half-integer  $BC_8$  and integer  $D_8$  vertex sets, with the right 5 overbar sets of 128 vertices being the negated vertices of the left 5 sets of 128 in reverse order.

It is these embeddings that have an isomorphic connection to  $\mathbb{U}$  and provide the  $E_8\leftrightarrow H_4(L\oplus R\oplus 1\oplus\varphi)$  mapping via  $\text{mapLR}$ . The *Mathematica*<sup>TM</sup> code for  $\text{mapLR}$  and the code to validate the  $E_8\leftrightarrow H_4$  isomorphism is shown in Appendix D Fig. 21. It demonstrates that  $E_8$  rotates into four 4D copies of  $H_4$  600-cells, with the original two (L)left side  $\varphi$  scaled 4D copies related to the two (R)right side unscaled 4D copies.

Due to the palindromic structure of  $\mathbb{U}$ , the  $H_{4L}$  and  $H_{4R}$  are also palindromic with each R vertex being the reverse order of the L vertex, along with  $\text{mapLR}$  exchanges in the (S)ub 24-cell vertices. For each L vertex that is not a member of the (T)etrahedral group's self-dual  $D_4$  24-cell (or  $\varphi T$ ), the R vertex will be a member of the scaled  $\varphi S$  (or S) respectively. This is due to the exchange of  $\varphi^{3/2}\leftrightarrow\varphi^{-3/2}$  in  $\text{mapLR}$  which changes the norm (i.e. to/from a large norm=1 or a small norm=1/ $\varphi$ ). The 24-cell T vertices are unaffected by  $\text{mapLR}$  exchange and have L and R vertex values of the palindromic opposite sign and the same norm.

It is clear that  $\mathbb{U}$  is traceless, but it is not unitary. Since  $\mathbb{U}$  is Hermitian, it is easily made unitary as  $e^{i\mathbb{U}}$ . While that is unitary it is not traceless, so it is not an  $A_7$  group  $SU(8)$  symmetry. For the identification of their palindromic characteristic polynomial coefficients, see Figs. 7-8.

See Appendix D Figs. 22-23 showing the detail of the  $E_8\leftrightarrow H_4(L\oplus R\oplus 1\oplus\varphi)$  isomorphism for each vertex.

## III. QUATERNIONIC WEYL ORBIT CONSTRUCTION

The content within this paper was generated using a computational environment the author has written in *Mathematica*<sup>TM</sup> by *Wolfram Research, Inc.*. In order to deal effectively with quaternions, it supplants the native

```
(* Show the Determinant of U=1 *)
Det@U
N[% /. φRep]
Out[*]=  $\frac{64 \varphi^9 - 64 \varphi^3}{256 \varphi^6}$ 
Out[*]= 1.

(* Show the Trace of U=0 *)
octSimplify /@ Tr@U
Chop@N[% /. φRep]
Out[*]=  $-\frac{1}{\varphi^{3/2}} - \sqrt{\frac{1}{\varphi}} + \sqrt{\varphi}$ 
Out[*]= 0

In[*]:= (* Show the Eigensystem of U *)
octSimplify /@ FullSimplify[Eigenvalues@U,
Assumptions → φAssumptions]
Total@N[% /. φRep]
FullSimplify[Eigenvectors@U, Assumptions → φAssumptions]
Out[*]=  $\left\{-\sqrt{\frac{1}{\varphi}}, -\sqrt{\frac{1}{\varphi}}, \sqrt{\frac{1}{\varphi}}, -\sqrt{\varphi}, \sqrt{\varphi}, \sqrt{\varphi}, -\sqrt{\varphi}, \sqrt{\frac{1}{\varphi}}\right\}$ 
Out[*]= 0.


$$\begin{pmatrix} 0 & -1 & 0 & 0 & 0 & 0 & 1 & 0 \\ 0 & 0 & -1 & -1 & 1 & 1 & 0 & 0 \\ 0 & 0 & -1 & 1 & -1 & 1 & 0 & 0 \\ 0 & 1 & -1 & 0 & 0 & -1 & 1 & 0 \\ 0 & 1 & 1 & 0 & 0 & 1 & 1 & 0 \\ 0 & 0 & 0 & 1 & 1 & 0 & 0 & 0 \\ 1 & 0 & 0 & 0 & 0 & 0 & 0 & 1 \\ -1 & 0 & 0 & 0 & 0 & 0 & 0 & 1 \end{pmatrix}$$


In[*]:= (* Get the Characteristic coefficients *)
FullSimplify[CharacteristicPolynomial[U, x],
Assumptions → φAssumptions]
Out[*]=  $\frac{1}{\varphi^{9/2}} (\varphi^3 x^7 (\varphi (1. - \varphi) + 1.) + \varphi^{3/2} (0.25 \varphi^6 - 0.25) +$ 
 $1. \varphi^{9/2} x^8 + \varphi^{3/2} (\varphi (\varphi (-0.25 \varphi^3 - 1. \varphi - 1.) - 2.) + 1.) + 0.25) x^6 +$ 
 $\varphi (\varphi (0.25 \varphi^6 - 0.25 \varphi^5 + 1. \varphi^4 - 1. \varphi^3 - 2. \varphi - 1.25) + 0.25) x^5 +$ 
 $\sqrt{\varphi} (\varphi (0.25 \varphi^7 + 0.25 \varphi^6 + 0.25 \varphi^5 + 1. \varphi^4 + 2. \varphi^3 + 0.75 \varphi - 1.25) - 0.25) x^4 +$ 
 $(\varphi (\varphi (\varphi (\varphi (-0.25 \varphi (1. \varphi - 1.) (1. \varphi^2 + 1.) - 1.) + 2.) + 1.25) + 0.75) + 0.25) - 0.25) x^3 +$ 
 $\sqrt{\varphi} (\varphi (\varphi (-0.25 \varphi^5 - 0.25 \varphi^4 - 0.25 \varphi^3 - 1. \varphi - 1.) + 1.25) + 0.25) + 0.25) x^2 +$ 
 $\varphi (0.25 \varphi^6 - 0.25 \varphi^5 - 1. \varphi - 0.25) + 0.25) x)$ 

In[*]:= (* Collect and compare them *)
((1 + σ x2) (1 - τ x2))2 /. s1Rep;
FullSimplify[% == %];
Expand@%;
Collect[% , x]
Out[*]=  $x^8 + \left(-2\varphi - \frac{2}{\varphi}\right)x^6 + \left(\varphi^2 + \frac{1}{\varphi^2} + 4\right)x^4 + \left(-2\varphi - \frac{2}{\varphi}\right)x^2 + 1$ 

In[*]:= (* The palindrome of coefficients in the characteristic
matrix of U *)
{1, 0, 2 (σ - τ), 0, 7, 0, 2 (σ - τ), 0, 1};
cU = 1 + 0 x + 2 (σ - τ) x2 + 0 x3 + 7 x4 + 0 x5 + 2 (σ - τ) x6 + 0 x7 + x8 /. s1Rep;
FullSimplify[% == %, Assumptions → φAssumptions]
Out[*]= φ2 x = (φ + 1) x

In[*]:= (* Verify the simplification is True *)
Chop@N[% /. φRep]
Out[*]= True
```

FIG. 7. The trace, determinant, Eigenvalues, Eigenvector matrix, and characteristic polynomial coefficients of U

```
]- octSimplify /@ FullSimplify[Eigenvalues@eIU, Assumptions → φAssumptions]
Total@N[% /. φRep]
FullSimplify[Eigenvectors@eIU, Assumptions → φAssumptions]
]-  $\{e^{-i\sqrt{\varphi}}, e^{i\sqrt{\varphi}}, e^{-i\sqrt{\varphi}}, e^{i\sqrt{\varphi}}, e^{-i\sqrt{\varphi}}, e^{i\sqrt{\varphi}}, e^{-i\sqrt{\varphi}}, e^{i\sqrt{\varphi}}\}$ 
]- 4.0037 + 0.i
]-  $\begin{pmatrix} 1 & 0 & 0 & 0 & 0 & 0 & 0 & 1 \\ -1 & 0 & 0 & 0 & 0 & 0 & 0 & 1 \\ 0 & -1 & 0 & 0 & 0 & 0 & 1 & 0 \\ 0 & 0 & -1 & -1 & 1 & 1 & 0 & 0 \\ 0 & 0 & -1 & 1 & -1 & 1 & 0 & 0 \\ 0 & 1 & -1 & 0 & 0 & -1 & 1 & 0 \\ 0 & 1 & 1 & 0 & 0 & 1 & 1 & 0 \\ 0 & 0 & 0 & 1 & 1 & 0 & 0 & 0 \end{pmatrix}$ 
]- cF1 = Cos[ $\frac{1}{\sqrt{\varphi}}$ ] + Cos[ $\sqrt{\varphi}$ ];
]- cF2 = Cos[ $\frac{1}{\sqrt{\varphi}}$ ] Cos[ $\sqrt{\varphi}$ ];
]- cF3 = Cos[ $\frac{1}{\sqrt{\varphi}}$ ]2 Cos[ $\sqrt{\varphi}$ ] + Cos[ $\frac{1}{\sqrt{\varphi}}$ ] Cos[ $\sqrt{\varphi}$ ]2;
]- cF4 = Cos[ $\frac{1}{\sqrt{\varphi}}$ ]2 + Cos[ $\sqrt{\varphi}$ ]2;
]- (* The palindrome of coefficients in the characteristic matrix of eIU *)
{1, -4 cF1, 4 (1 + 4 cF2 + cF4), -4 (3 cF1 + 4 cF3), 2 (3 + 4 (cF4 + 2 cF2 (cF2 + 2))), -4 (3 cF1 + 4 cF3), 4 (1 + 4 cF2 + cF4), -4 cF1, 1};
cIU = 1 - 4 cF1 x + 4 (1 + 4 cF2 + cF4) x2 - 4 (3 cF1 + 4 cF3) x3 + 2 (3 + 4 (cF4 + 2 cF2 (cF2 + 2))) x4 - 4 (3 cF1 + 4 cF3) x5 + 4 (1 + 4 cF2 + cF4) x6 - 4 cF1 x7 + x8 /. s1Rep;
N[% /. φRep]
]- x8 - 4.0037 x7 + 9.67125 x6 - 15.3419 x5 + 18.0346 x4 - 15.3419 x3 + 9.67125 x2 - 4.0037 x + 1.
]- (* Result 1 *)
FullSimplify[Re@eIU, Assumptions → φAssumptions] // MatrixForm
]- (* Result 2 *)
FullSimplify[Im@eIU, Assumptions → φAssumptions] // MatrixForm
]- (* Result 3 *)
FullSimplify[Tr@eIU, Assumptions → φAssumptions] // MatrixForm
]- (* Result 4 *)
FullSimplify[Chop@N[% /. φRep], Assumptions → φAssumptions] // MatrixForm
]- (* Result 5 *)
FullSimplify[Re@eIU /. φRep, Assumptions → φAssumptions] // MatrixForm
]- (* Result 6 *)
FullSimplify[Im@eIU /. φRep, Assumptions → φAssumptions] // MatrixForm
```

FIG. 8. The Eigenvalues, Eigenvector matrix, and characteristic polynomial coefficients of the unitary form of U as  $e^{iU}$  showing a  $\text{Tr@Re@}e^{iU} \approx 4$  and a traceless imaginary part

Quaternion package with a more flexible symbolic octonion ( $\mathbb{O}$ ) capability. This allows for the selection of a multiplication table from any of the 480 possible octonion tables, including their split and bi-octonion forms. It also handles the sedenion forms as well and has been used to verify the octonion forms of  $E_8$  from Koca[1], Dixon[15], Pushpa and Bisht[16], R. A. Wilson, Dray, and Monague[17], including the complexified octonions

of Günaydin-Gürsey[18] and Furey[19]. To ensure that our quaternion (and bi-quaternion) math is consistent with the standard multiplication convention related to quaternions, we need to select one of the 48 octonions with a first triad of 123 and a Cayley-Dickson construction where  $e_4$ - $e_7$  quadrant multiplication remains within the quadrant. See Fig. 9 showing the selected triads, Fano plane, and multiplication table of the octonion used in this and several of the referenced papers<sup>1</sup>.

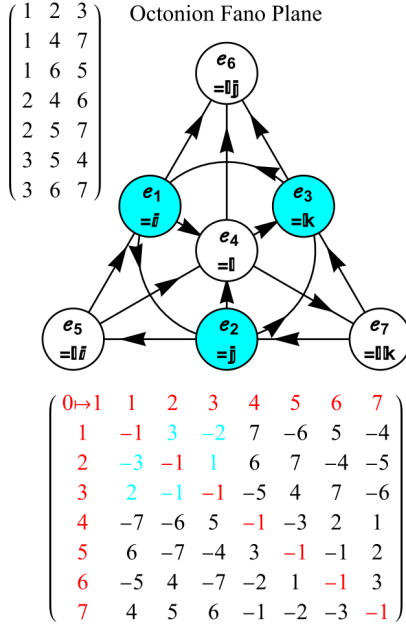


FIG. 9. The selected octonion Fano plane mnemonic and multiplication table based on its 7 structure constant triads. The first triad (123) defines standard convention for quaternions.

It has been shown that the 3D symmetry groups of  $A_3$ ,  $B_3$ , and  $H_3$ [3] and 4D symmetry groups of  $A_4$ ,  $D_4$ ,  $F_4$ , and  $H_4$  are related to the higher dimensional groups of  $D_6$  and  $E_8$ [5][9]. A quaternionic Weyl group orbit  $O(\Lambda)=W(H_4)=I$  of order 120 can be constructed from  $H_3$  which generates some of the Platonic, Archimedean and dual Catalan solids shown in Appendix B Fig. 18, including their irregular and chiral forms[4]. The polytopes for a particular orbit of  $O(\Lambda)=W(\text{group})$  are generated using a function  $\Lambda[\text{group}_-, \text{orbit}_-, \text{perm}_- : \text{"Rotate"}]$ , where **perm** can be one of 18 combinations of sign and position permutation functions (e.g. "oSign" gives all odd sign permutations and cyclic rotations of position and the default "Rotate" gives all sign permutations of cyclicly rotated positions). The first column in these figures show

<sup>1</sup> It is interesting to note that this particular octonion is close to (but not) palindromic. Using an algorithmic identification and construction of all of the possible 480 unique permutations of octonions[20], we find that a small change in triads to {123,145,167,264,257,347,356} with 5↔7 ordering swaps creates a palindromic  $E_8$ . This octonion is shown in Fig. 10

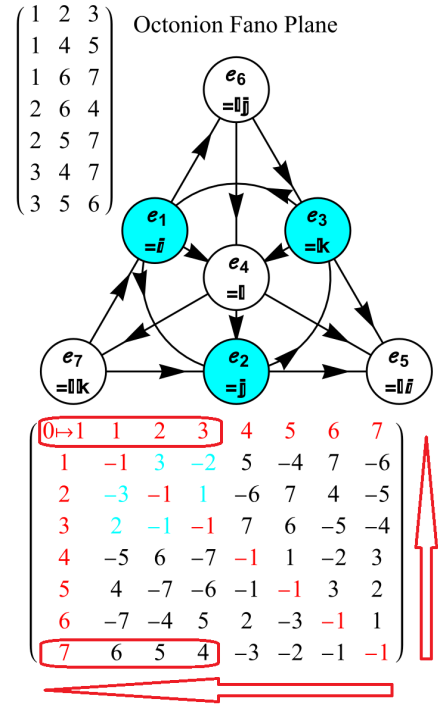


FIG. 10. An alternative set of structure constant triads, octonion Fano plane mnemonic, and multiplication table, with decorations showing the palindromic multiplication.

the set of calls to the  $\Lambda$  function. This same method is used to generate the  $H_4$ -based 4-polytopes of the 120-cell and 600-cell shown in Appendix A Figs. 14-16.

The  $A_3$  in  $A_4$  group embedding of  $SU(5) \supset SU(4) \otimes U_1$ [5] are shown in Appendix C Fig. 20 in combination with these 3 and 4-polytope visualizations.<sup>2</sup>

We identify the parent orbit (1000) of  $W(D_4)$  as the self-dual 24-cell T, which is the combination of the 4D octahedron (aka. 16-cell) and the 4D cube (aka. 8-cell with a 3D hull of the cuboctahedron derived from the truncated (0001)  $W(BC_4)$ ). T' is identified as the set of 3 orbits {(0100), (0010), (0001)} of  $W(D_4)$  with 8 vertices each made of 2-component (vector) quaternions and has a 3D hull of the rhombic dodecahedron. See Fig. 11 for their specific symbolic and numeric values.

From T (and T') we can take any one vertex to define a  $c$  (and  $c'=cp$ ) respectively. For this paper, we use as an example  $c=t_1$  from eq. (18) from Koca[3] which is our 13'th T (and T') shown in Fig.11 such that  $c=\frac{1}{2}(1+e_1-e_2-e_3)$  (and  $c'=\frac{e_2-e_3}{\sqrt{2}}$ ). Here  $c'$  is used with  $A'$  to generate the parent  $W(A_4)$ , or simply  $A$  as the 5-cell[3]. Specifically,  $A=(c' \circ A')^*$  with

<sup>2</sup> In the methods and coding descriptions, since Mamone[6] identifies the 5-cell as S, but Koca uses S to identify the (S)ub 24-cell (a convention which we use here), Mamone's  $A_4$ -based 5-cell is now identified as A which is the 4D version of the tetrahedron.

```
(* Show T vertices *)
checkVertices[T, False, True, True, False, False, False]
Out[*]= List length= 24 and it is symbolic octonion
```

Math =	$\begin{pmatrix} 1 & \frac{1}{2}(-1 - e_1 - e_2 - e_3) \\ 2 & \frac{1}{2}(-1 - e_1 - e_2 + e_3) \\ 3 & \frac{1}{2}(-1 - e_1 + e_2 - e_3) \\ 4 & \frac{1}{2}(-1 - e_1 + e_2 + e_3) \\ 5 & \frac{1}{2}(-1 + e_1 - e_2 - e_3) \\ 6 & \frac{1}{2}(-1 + e_1 - e_2 + e_3) \\ 7 & \frac{1}{2}(-1 + e_1 + e_2 - e_3) \\ 8 & \frac{1}{2}(-1 + e_1 + e_2 + e_3) \\ 9 & \frac{1}{2}(1 - e_1 - e_2 - e_3) \\ 10 & \frac{1}{2}(1 - e_1 - e_2 + e_3) \\ 11 & \frac{1}{2}(1 - e_1 + e_2 - e_3) \\ 12 & \frac{1}{2}(1 - e_1 + e_2 + e_3) \\ 13 & \frac{1}{2}(1 + e_1 - e_2 - e_3) \\ 14 & \frac{1}{2}(1 + e_1 - e_2 + e_3) \\ 15 & \frac{1}{2}(1 + e_1 + e_2 - e_3) \\ 16 & \frac{1}{2}(1 + e_1 + e_2 + e_3) \\ 17 & -e_3 \\ 18 & -e_2 \\ 19 & -e_1 \\ 20 & -1 \\ 21 & e_3 \\ 22 & e_2 \\ 23 & e_1 \\ 24 & 1 \end{pmatrix}$	Numeric =	$\begin{pmatrix} 1 & -0.5 & 0.5 & e_1 - 0.5 & e_2 & 0.5 & e_3 \\ 2 & -0.5 & -0.5 & e_1 - 0.5 & e_2 + 0.5 & e_3 \\ 3 & -0.5 & -0.5 & e_1 + 0.5 & e_2 - 0.5 & e_3 \\ 4 & -0.5 & 0.5 & e_1 + 0.5 & e_2 + 0.5 & e_3 \\ 5 & -0.5 & 0.5 & e_1 - 0.5 & e_2 & 0.5 & e_3 \\ 6 & -0.5 & 0.5 & e_1 - 0.5 & e_2 + 0.5 & e_3 \\ 7 & -0.5 & -0.5 & e_1 + 0.5 & e_2 - 0.5 & e_3 \\ 8 & -0.5 & -0.5 & e_1 + 0.5 & e_2 + 0.5 & e_3 \\ 9 & 0.5 & -0.5 & e_1 - 0.5 & e_2 - 0.5 & e_3 \\ 10 & 0.5 & -0.5 & e_1 - 0.5 & e_2 + 0.5 & e_3 \\ 11 & 0.5 & -0.5 & e_1 + 0.5 & e_2 - 0.5 & e_3 \\ 12 & 0.5 & -0.5 & e_1 + 0.5 & e_2 + 0.5 & e_3 \\ 13 & 0.5 & 0.5 & e_1 - 0.5 & e_2 - 0.5 & e_3 \\ 14 & 0.5 & 0.5 & e_1 - 0.5 & e_2 + 0.5 & e_3 \\ 15 & 0.5 & 0.5 & e_1 + 0.5 & e_2 - 0.5 & e_3 \\ 16 & 0.5 & 0.5 & e_1 + 0.5 & e_2 + 0.5 & e_3 \\ 17 & 0 & -1 & e_3 \\ 18 & 0 & -1 & e_2 \\ 19 & 0 & -1 & e_1 \\ 20 & 0 & 1 & e_1 \\ 21 & 0 & 1 & e_3 \\ 22 & 0 & 1 & e_2 \\ 23 & 0 & 1 & e_1 \\ 24 & 0 & 1 & 1 \end{pmatrix}$
--------	---	-----------	--

```
(* Show T' vertices *)
checkVertices[Tp, False, True, True, False, False, False]
Out[*]= List length= 24 and it is symbolic octonion
```

Math =	$\begin{pmatrix} 1 & \frac{1+e_1}{\sqrt{2}} \\ 2 & \frac{1+e_2}{\sqrt{2}} \\ 3 & \frac{1+e_3}{\sqrt{2}} \\ 4 & \frac{1+e_3}{\sqrt{2}} \\ 5 & \frac{1+e_2}{\sqrt{2}} \\ 6 & \frac{1+e_1}{\sqrt{2}} \\ 7 & -\frac{e_1+e_2}{\sqrt{2}} \\ 8 & -\frac{e_1+e_3}{\sqrt{2}} \\ 9 & -\frac{e_1+e_3}{\sqrt{2}} \\ 10 & -\frac{e_1+e_2}{\sqrt{2}} \\ 11 & -\frac{e_2+e_3}{\sqrt{2}} \\ 12 & -\frac{e_2+e_3}{\sqrt{2}} \\ 13 & \frac{e_2-e_3}{\sqrt{2}} \\ 14 & \frac{e_2+e_3}{\sqrt{2}} \\ 15 & \frac{e_1-e_2}{\sqrt{2}} \\ 16 & \frac{e_1-e_3}{\sqrt{2}} \\ 17 & \frac{e_1+e_3}{\sqrt{2}} \\ 18 & \frac{e_1+e_2}{\sqrt{2}} \\ 19 & -\frac{1+e_1}{\sqrt{2}} \\ 20 & -\frac{1+e_2}{\sqrt{2}} \\ 21 & -\frac{1+e_3}{\sqrt{2}} \\ 22 & \frac{1+e_3}{\sqrt{2}} \\ 23 & \frac{1+e_2}{\sqrt{2}} \\ 24 & \frac{1+e_1}{\sqrt{2}} \end{pmatrix}$	Numeric =	$\begin{pmatrix} 1 & -0.70711 & -0.70711 & e_1 \\ 2 & -0.70711 & -0.70711 & e_2 \\ 3 & -0.70711 & -0.70711 & e_3 \\ 4 & 0.70711 & +0.70711 & e_3 \\ 5 & -0.70711 & +0.70711 & e_2 \\ 6 & -0.70711 & +0.70711 & e_1 \\ 7 & 0 & -0.70711 & e_1 - 0.70711 & e_2 \\ 8 & 0 & -0.70711 & e_1 & 0.70711 & e_3 \\ 9 & 0 & -0.70711 & e_1 & 0.70711 & e_3 \\ 10 & 0 & -0.70711 & e_1 & 0.70711 & e_2 \\ 11 & 0 & -0.70711 & e_2 & 0.70711 & e_3 \\ 12 & 0 & -0.70711 & e_2 & 0.70711 & e_3 \\ 13 & 0 & +0.70711 & e_2 & 0.70711 & e_3 \\ 14 & 0 & +0.70711 & e_2 & 0.70711 & e_3 \\ 15 & 0 & -0.70711 & e_1 & -0.70711 & e_2 \\ 16 & 0 & +0.70711 & e_1 & -0.70711 & e_3 \\ 17 & 0 & +0.70711 & e_1 & 0.70711 & e_3 \\ 18 & 0 & +0.70711 & e_1 & 0.70711 & e_2 \\ 19 & 0.70711 & -0.70711 & e_1 \\ 20 & 0.70711 & -0.70711 & e_2 \\ 21 & 0.70711 & -0.70711 & e_3 \\ 22 & 0.70711 & +0.70711 & e_3 \\ 23 & 0.70711 & +0.70711 & e_2 \\ 24 & 0.70711 & +0.70711 & e_1 \end{pmatrix}$
--------	--	-----------	--

FIG. 11. The values of the  $D_4$  24-cell T and its alternate  $T'$ 

```
In[*]= (* Generate the A' parent Weyl orbit *)
AA4[{0, 1, 4, 2, 3}, {1, 0, 0, 0}]
```

$$\text{Out[*]} = \begin{pmatrix} -\frac{1}{\sqrt{2}} & 0 & \frac{\varphi}{\sqrt{10}} & \frac{1}{\sqrt{10}\varphi} \\ \frac{1}{\sqrt{2}} & 0 & \sqrt{\frac{2}{5}}\varphi - \frac{\varphi}{\sqrt{10}} & \frac{\sqrt{\frac{2}{5}}}{\varphi} - \frac{1}{\sqrt{10}\varphi} \\ 0 & -\frac{1}{\sqrt{2}} & \frac{\varphi^2}{\sqrt{10}} - \sqrt{\frac{2}{5}}\varphi & -\frac{1}{\sqrt{10}\varphi^2} - \frac{\sqrt{\frac{2}{5}}}{\varphi} \\ 0 & \frac{1}{\sqrt{2}} & \sqrt{\frac{2}{5}} - \frac{\varphi^2}{\sqrt{10}} & \frac{1}{\sqrt{10}\varphi^2} - \sqrt{\frac{2}{5}} \\ 0 & 0 & -\sqrt{\frac{2}{5}} & \sqrt{\frac{2}{5}} \end{pmatrix} \text{NoneNoSign}$$

```
In[*]= (* Scale by -\frac{\sqrt{5}}{2} to match conventional A scaling *)
Aplist = oct2List@biQuaternion[-\frac{\sqrt{5}}{2} #] & /@%[[1, 1]]
```

$$\text{Out[*]} = \begin{pmatrix} \frac{\sqrt{5}}{2} & 0 & -\frac{\varphi}{2\sqrt{2}} & \frac{1}{2\sqrt{2}\varphi} & 0 & 0 & 0 & 0 \\ -\frac{\sqrt{5}}{2} & 0 & -\frac{\varphi}{2\sqrt{2}} & -\frac{1}{2\sqrt{2}\varphi} & 0 & 0 & 0 & 0 \\ 0 & \frac{\sqrt{5}}{2} & \frac{\sqrt{2}\varphi}{2} & \frac{2\varphi+1}{2\sqrt{2}\varphi^2} & 0 & 0 & 0 & 0 \\ 0 & -\frac{\sqrt{5}}{2} & \frac{\sqrt{2}\varphi}{2} & \frac{2\varphi-1}{2\sqrt{2}\varphi^2} & 0 & 0 & 0 & 0 \\ 0 & 0 & \frac{1}{\sqrt{2}} & -\frac{1}{\sqrt{2}} & 0 & 0 & 0 & 0 \end{pmatrix}$$

```
In[*]= (* Put it into symbolic octonion form *)
Ap = octSimplify@octonion /@%;
% // MatrixForm
```

$$\text{Out[*]} // \text{MatrixForm} = \begin{pmatrix} -\frac{\varphi e_2}{2\sqrt{2}} - \frac{e_1}{2\sqrt{2}\varphi} + \frac{\sqrt{5}}{2} \\ -\frac{\varphi e_3}{2\sqrt{2}} - \frac{e_1}{2\sqrt{2}\varphi} - \frac{\sqrt{5}}{2} \\ \frac{\varphi e_2}{2\sqrt{2}} - \frac{e_1}{2\sqrt{2}\varphi} + \frac{\sqrt{5}}{2} \\ \frac{\varphi e_3}{2\sqrt{2}} - \frac{e_1}{2\sqrt{2}\varphi} - \frac{\sqrt{5}}{2} \\ \frac{(\varphi^2-2)e_2}{2\sqrt{2}} - \frac{(\varphi^2-2)e_3}{2\sqrt{2}} + \frac{1}{2}\sqrt{\frac{5}{2}}e_1 \\ \frac{\varphi e_2}{\sqrt{2}} - \frac{e_1}{\sqrt{2}} \end{pmatrix}$$

```
In[*]= (* Display vertex value *)
checkVertices[% , False, True, True, False, False, False]
```

```
Out[*]= List length= 5 and it is symbolic octonion
```

$$\text{Math} = \begin{pmatrix} 1 & \frac{1}{4}(1+\sqrt{5})^2 e_2 + \frac{1}{2}\sqrt{5}(1+\sqrt{5}) \\ 2 & \frac{1}{4}(1+\sqrt{5})^2 e_2 + \frac{1}{2}\sqrt{5}(1+\sqrt{5}) \\ 3 & \sqrt{\frac{1}{4}(1+\sqrt{5})^2 e_1 - \frac{1}{4}(1+\sqrt{5})^2} \left[ -2\frac{1}{2}(1+\sqrt{5})e_2 + 2e_3 \right] \\ 4 & \frac{\sqrt{2}(1+\sqrt{5})^2}{(1+\sqrt{5})^2} \left[ -\sqrt{5}e_1(-2\frac{1}{2}(1+\sqrt{5})e_2 + 2e_3) \right] \\ 5 & \frac{e_2 - e_3}{\sqrt{2}} \end{pmatrix}$$

```
Out[*]= List length= 5 and it is symbolic octonion
```

$$\text{Numeric} = \begin{pmatrix} 1 & -0.57206 e_2 - 0.21851 e_3 + 0.79057 \\ 2 & -0.57206 e_2 - 0.21851 e_3 - 0.79057 \\ 3 & 0.79057 e_1 + 0.21851 e_2 + 0.57206 e_3 + 0. \\ 4 & -0.79057 e_1 + 0.21851 e_2 + 0.57206 e_3 + 0. \\ 5 & 0.70711 e_2 - 0.70711 e_3 + 0. \end{pmatrix}$$

```
In[*]= (* Simplify quaternion multiplication using prqr which also handles lists,
We scale up/down by 4 for symbolic clarity.
Please note the double struck A to avoid stepping on LieArt *)
A = \frac{1}{4} octonion@biQuaternion[# # . qRep] * / . slRep & /@
(* qRep replaces the symbolic forms \varphi \rightarrow (\sqrt{5}+1)/2, also note the conjugation
(4 oct2Quat @ # & /@ Flatten@prq[cp, 1, Ap]);
In[*]= checkVertices[A /. e_0 -> 1, False, True, True, False, False, False]
```

```
Out[*]= List length= 5 and it is symbolic octonion
```

$$\text{Math} = \begin{pmatrix} 1 & \frac{1}{4}(\sqrt{5} e_1 - \sqrt{5} e_2 + \sqrt{5} e_3 + 1) \\ 2 & \frac{1}{4}(\sqrt{5} e_1 + \sqrt{5} e_2 - \sqrt{5} e_3 + 1) \\ 3 & \frac{1}{4}(-\sqrt{5} e_1 + \sqrt{5} e_2 + \sqrt{5} e_3 + 1) \\ 4 & \frac{1}{4}(-\sqrt{5} e_1 - \sqrt{5} e_2 - \sqrt{5} e_3 + 1) \\ 5 & -1 \end{pmatrix}$$

$$\text{Numeric} = \begin{pmatrix} 1 & 0.55902 e_1 - 0.55902 e_2 + 0.55902 e_3 + 0.25 \\ 2 & 0.55902 e_1 + 0.55902 e_2 - 0.55902 e_3 + 0.25 \\ 3 & -0.55902 e_1 + 0.55902 e_2 + 0.55902 e_3 + 0.25 \\ 4 & -0.55902 e_1 - 0.55902 e_2 - 0.55902 e_3 + 0.25 \\ 5 & -1 \end{pmatrix}$$
FIG. 12. Explicit *Mathematica*<sup>TM</sup> computation of A from the  $\Lambda A_4[\Lambda, \text{orbit}_-]$  generated A'

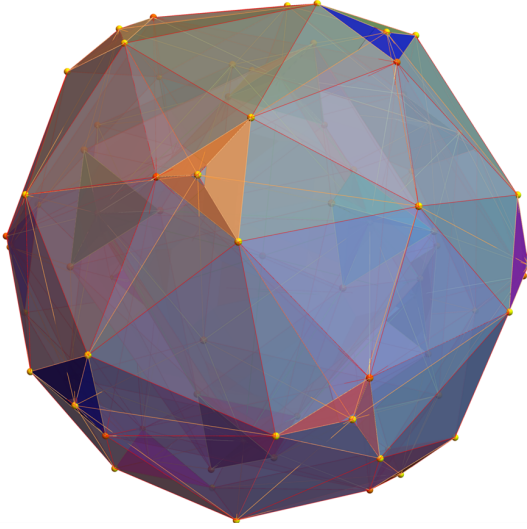


FIG. 13. Visualization of the 144 root vertices of  $S'+T+T'$  now identified as the dual snub 24-cell

$A' = \Lambda A4[\{0, 1, 4, 2, 3\}, \{1, 0, 0, 0\}]$ .<sup>3</sup> See Fig. 12 for the explicit *Mathematica*<sup>TM</sup> computation related to  $A$  and  $A'$ .

The snub orbit (0000) of  $W(D_4)$  will generate the vertices of the snub 24-cell or  $S=I-T$ , as with the alternate snub 24-cell  $S'=I'-T'$  as shown in (7) and (8). We can generate  $S$  (or  $S'$ ) by taking the odd (or even) sign and cyclic position permutations of a seed quaternion  $p \in I$  (or  $I'$ ) to be assigned to  $\alpha$  (or  $\beta$ ) for generating  $S$  (or  $S'$ ) respectively. There are only 48 that satisfy the necessary constraint where  $p^5 = \pm 1$ . Those quaternions that satisfy the constraint are identified with an \* in Appendix D. For this paper, we took the 8'th permutation of the generated  $S$  for  $\alpha = \frac{1}{2} \left( \frac{1}{\varphi} + \varphi e_2 + e_1 \right)$  (and  $S'$  for  $\beta = \frac{-\varphi - \frac{e_2 + \sqrt{5}e_1}{\sqrt{8}}}{\sqrt{8}}$ ). This process of generating the snub 24-cell can be visualized as generating four quaternion 4D rotations of  $T$  (and  $T'$ ). The 3D hulls of  $I'$  is shown in Fig. 15.

<sup>3</sup> The 4-polytopes for a particular orbit of  $O(\Lambda)=W(\text{group})$  are generated using a function  $\Lambda[\text{group\_}, \text{orbit\_}, \text{perm\_}]$  which is called by  $\Lambda A4[\Lambda\_ , \text{orbit\_}]$  for the subgroup embeddings in  $A_4$  as described in [5]. In addition, `SmallCircle` (`o`) is the symbolic operator for quaternion (octonion) multiplication that operates across lists, along with the expected symbolic exponentials (`*` and `†`) for Conjugate and ConjugateTranspose respectively. The function `prq[p_., r_., q_., left:False] := If[left, q o (p o r), p o (r o q)]` implements the operation of  $[p, q]:r$  from eq. (6) in [3], which is defined for any combinations of inputs as elements or lists in order to add flexibility to quaternion and octonion operators, including left or right (default) non-commutative multiplication ordering. Other operators are also available for scalar product+ ( $\oplus$ ), scalar product- ( $\ominus$ ), commutator ( $\odot$ ), anti-commutator ( $\wedge$ ), derivation ( $\square$ ), Kronecker product ( $\otimes$ ), and `octExp` for exponential powers of octonions.

$$\begin{aligned} S &= I - T = \sum_{i=1}^4 \alpha^i \circ T \\ \text{or} \\ I &= \text{prq}[\alpha^{0-4}, 1, T] \end{aligned} \quad (7)$$

$$\begin{aligned} S' &= I' - T' = \sum_{i=1}^4 \beta^i \circ T' \\ \text{or} \\ I' &= \text{prq}[\beta^{0-4}, 1, T'] \end{aligned} \quad (8)$$

The 3D hulls for one copy of  $I$  (or  $\varphi I$ ) are represented in Fig. 14 hulls  $\{2,3,5\}$  (or  $\{6,7,8\}$ ) respectively plus  $1/2$  of the vertices in hull 4. The vertex values of  $I$  are listed in either of the center columns of either Appendix D Fig. 22 or Fig. 23.

Koca[3] has also identified the dual to the snub 24-cell as being made up of the 144 root vertices of  $S'+T+T'$ . This 4-polytope is visualized in Fig. 13.

The equations for the generation of  $J$  (and  $J'$ ) are shown in (9) and (10). As it was for  $I$  (and  $I'$ ) vertices each mapping to 5 quaternion rotations of  $T$  (and  $T'$ ),  $J$  (and  $J'$ ) vertices each map to 5 quaternion rotations of  $I$  (and  $I'$ ) or 25 quaternion rotations of  $T$  (and  $T'$ ). Given the isomorphism between each  $E_8$  root vertex and 4 copies of  $I$  (i.e.  $L$  and  $R$  each at unit and  $1/\varphi$  scales) as demonstrated in Section II, this means quaternionic Weyl orbit construction, when used with  $\mathbb{U}$  and `mapLR`, provides for an explicit map between each of the 240  $E_8$  root vertices and 20  $J$  (or  $J'$ ) vertices (i.e.  $20=4 L \oplus R \oplus 1 \oplus \varphi$  copies of each  $I$  (or  $I'$ ) vertex  $\otimes 5$  quaternion rotations).

$$\begin{aligned} J &= \sum_{i=0}^4 c' \circ \bar{\alpha}^{\dagger i} \circ \alpha^i \circ T \\ \text{or} \\ J &= \text{prq}[A', \alpha^{0-4}, T] \end{aligned} \quad (9)$$

$$\begin{aligned} J' &= \sum_{i=0}^4 c \circ \bar{\beta}^{\dagger i} \circ \beta^i \circ T' \\ \text{or} \\ J' &= \text{prq}[A', \beta^{0-4}, T'] \end{aligned} \quad (10)$$

See Figs. 16-17 for the 120-cell ( $J$ ) and its alternate ( $J'$ ) as generated by  $J=\text{prq}[A', 1, I]$  and  $J'=\text{prq}[A', 1, I']$  respectively.

#### IV. CONCLUSION

This paper has given an explicit isomorphic mapping from the 240  $\mathbb{R}^8$  root  $E_8$  Gossett  $4_{21}$  8-polytope to two  $\varphi$  scaled copies of the 120 root  $H_4$  600-cell quaternion 4-polytope using  $\mathbb{U}$ . It has also shown the inverse map from a single  $H_4$  600-cell to  $E_8$  using a  $4D \leftrightarrow 8D$  chiral  $L \leftrightarrow R$  mapping function,  $\varphi$  scaling, and  $\mathbb{U}^{-1}$ . This approach has shown that there are actually four copies of each 600-cell living within  $E_8$  in the form of chiral  $H_{4L} \oplus \varphi H_{4L} \oplus H_{4R} \oplus \varphi H_{4R}$  roots. In addition, it has



demonstrated a quaternion Weyl orbit construction of  $H_4$ -based 4-polytopes that provides an explicit map from  $E_8$  to four copies of the tri-rectified Coxeter-Dynkin diagram of  $H_4$ , namely the 120-cell of order 600. Taking advantage of this property promises to open the door to as yet unexplored chiral  $E_8$ -based Grand Unified Theories or GUTs. It is anticipated that these visualizations and connections will be useful in discovering new insights

into unifying the mathematical symmetries as they relate to unification in theoretical physics.

## ACKNOWLEDGMENTS

I would like to thank my wife for her love and patience and those in academia who have taken the time to review this work.

- 
- [1] M. Koca, E8 Lattice with Octonions and Icosians, CERN, 1211 Geneva 23, Switzerland (1989).
- [2] M. Koca and N. Koca, Quaternionic Roots of E8 Related Coxeter Graphs and Quasicrystals, *Turkish Journal of Physics* **22**, 421 (1998).
- [3] M. Koca, M. Al-Ajmi, and N. O. Koca, Quaternionic representation of snub 24-cell and its dual polytope derived from e8 root system, *Linear Algebra and its Applications* **434**, 977 (2011).
- [4] M. Koca, N. O. Koca, and M. Al-Shueili, Chiral Polyhedra Derived From Coxeter Diagrams and Quaternions, ArXiv e-prints math.ph (2011), [arXiv:1006.3149 \[math-ph\]](https://arxiv.org/abs/1006.3149).
- [5] M. Koca, N. O. Koca, and M. Al-Ajmi, 4d-polytopes and their dual polytopes of the coxeter group a4 represented by quaternions, *International Journal of Geometric Methods in Modern Physics* **09**, 1250035 (2012).
- [6] S. Mamone, G. Pileio, and M. H. Levitt, Orientational sampling schemes based on four dimensional polytopes, *Symmetry* **2**, 1423 (2010).
- [7] J. H. Conway, R. H. Hardin, and N. J. A. Sloane, Packing Lines, Planes, etc.: Packings in Grassmannian Space, ArXiv e-prints math.CO (2002), [arXiv:math/0208004 \[math.CO\]](https://arxiv.org/abs/math/0208004).
- [8] D. A. Richter, Triacontagonal coordinates for the E8 root system, ArXiv e-prints math.GM (2007), [arXiv:0704.3091 \[math.GM\]](https://arxiv.org/abs/0704.3091).
- [9] P. P. Dechant, The birth of E8 out of the spinors of the icosahedron, *Proceedings of the Royal Society of London Series A* **472**, 20150504 (2016), [arXiv:1602.05985 \[math-ph\]](https://arxiv.org/abs/1602.05985).
- [10] J. C. Baez, From the Icosahedron to E8, ArXiv e-prints math.HO (2017), [arXiv:1712.06436 \[math.HO\]](https://arxiv.org/abs/1712.06436).
- [11] J. G. Moxness, The 3D Visualization of E8 using an H4 Folding Matrix, [www.vixra.org/abs/1411.0130](https://www.vixra.org/abs/1411.0130) (2014).
- [12] J. G. Moxness, Mapping the fourfold H4 600-cells emerging from E'8, [www.vixra.org/abs/1808.0107](https://www.vixra.org/abs/1808.0107) (2018).
- [13] J. G. Moxness, Unimodular rotation of E'8 to H'4 600-cells, [www.vixra.org/abs/1910.0345](https://www.vixra.org/abs/1910.0345) (2019).
- [14] J. G. Moxness, 3D Polytope Hulls of E8 4'21, 2'41, and 1'42, [www.vixra.org/abs/2005.0200](https://www.vixra.org/abs/2005.0200) (2020).
- [15] G. Dixon, Integral octonions, octonion xy-product, and the leech lattice, ArXiv e-prints math.th (2010), [arXiv:1011.2541 \[hep-th\]](https://arxiv.org/abs/1011.2541).
- [16] Pushpa, P. S. Bisht, T. Li, and O. P. S. Negi, Quaternion octonion reformulation of grand unified theories, *International Journal of Theoretical Physics* **51**, 3228 (2012).
- [17] R. A. Wilson, T. Dray, and C. A. Manogue, An octonionic construction of e8 and the lie algebra magic square, *Innovations in Incidence Geometry: Algebraic, Topological and Combinatorial* **20**, 611 (2023).
- [18] M. Günaydin and F. Gürsey, Quark structure and octonions, *Journal of Mathematical Physics* **14**, 1651 (2003), [https://pubs.aip.org/aip/jmp/article-pdf/14/11/1651/8805448/1651\\_1\\_online.pdf](https://pubs.aip.org/aip/jmp/article-pdf/14/11/1651/8805448/1651_1_online.pdf).
- [19] C. Furey,  $Su(3)_c \times su(2)_l \times u(1)_y (\times u(1)_x)$  as a symmetry of division algebraic ladder operators, *The European Physical Journal C* **78**, 10.1140/epjc/s10052-018-5844-7 (2018).
- [20] J. G. Moxness, The Comprehensive Split Octonions and their Fano Planes, [theoryofeverything.org/TOE/JGM/splitFano.pdf](https://theoryofeverything.org/TOE/JGM/splitFano.pdf) (2013).
- [21] R. M. Fonseca, GroupMath: A mathematica package for group theory calculations, *Computer Physics Communications* **267**, 108085 (2021).
- [22] P. Grozman and D. Leites, Lie superalgebra structures, *Czechoslovak Journal of Physics* **54**, 1313 (2004).

**Appendix A: Concentric hulls from Platonic 3D projection with numeric and symbolic norm distances**  
Figs. 14-17

**Appendix B: Archimedean and dual Catalan solids**  
Fig. 18

**Appendix C: Maximal  $SO(16)=D_8$  related embeddings of  $E_8$  at height 248**  
Figs. 19-20

**Appendix D: Mathematica<sup>TM</sup> code and output showing  $E_8 \leftrightarrow H_4$  isomorphism**  
Figs. 21-23

ListName= C60atE8

Dims used={1, 2, 3}  
 tallyList={4, 24, 40, 48}  
 {30, 40, 24, 30}

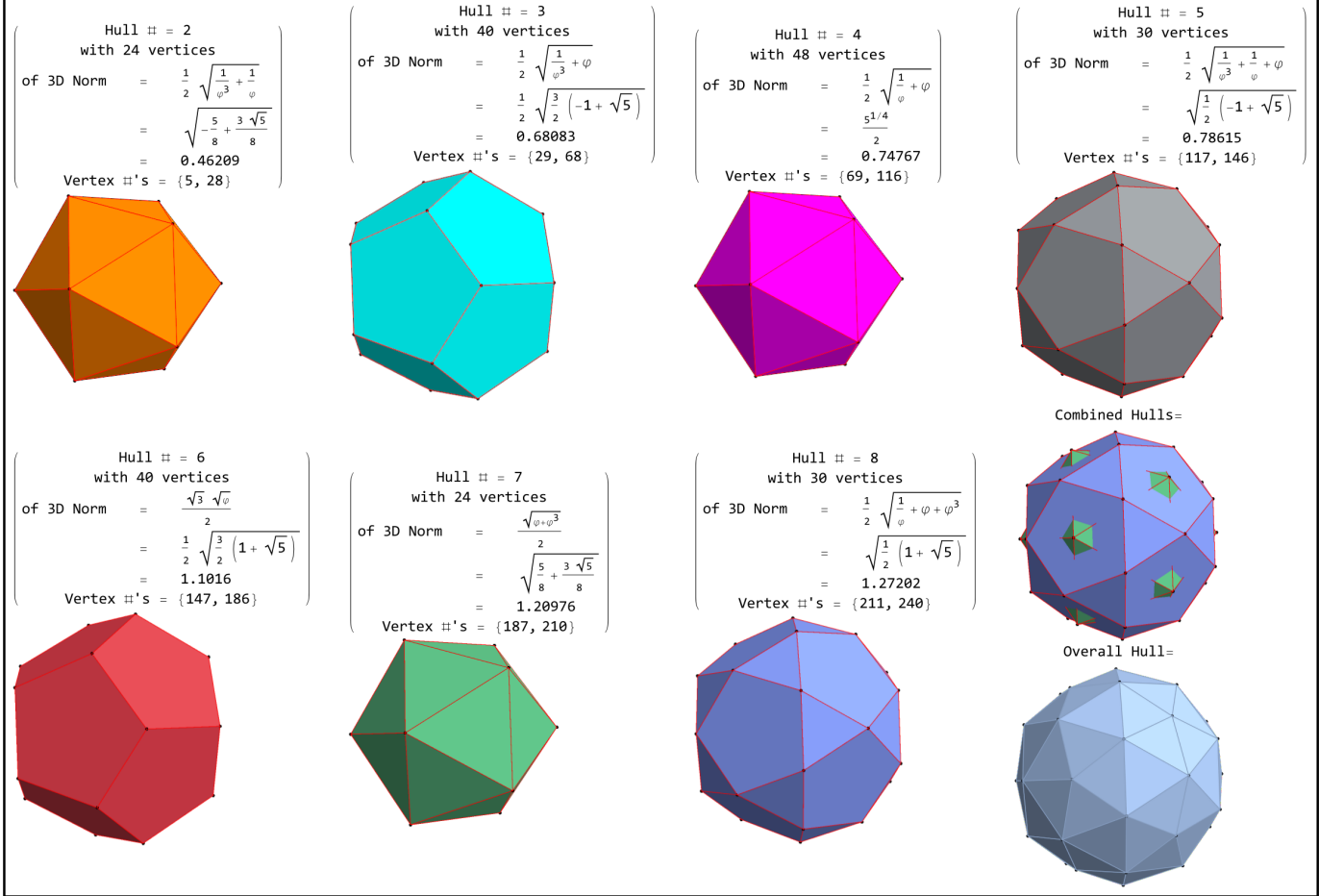


FIG. 14. Concentric hulls of  $4_{21}$  in Platonic 3D projection with numeric and symbolic norm distances

```

In[ ]:=
Ip = Flatten@prq[octExpa, 1, Tp];
IpRnd = rndOct /@%;
IpList = oct2List@# & /@%%;
hulls3DPerms["IpList", False, , 1]
ListName= IpList

```

Dims used={1, 2, 3}  
 tallyList={8, 8, 12, 24}  
 {24, 24, 8, 12}

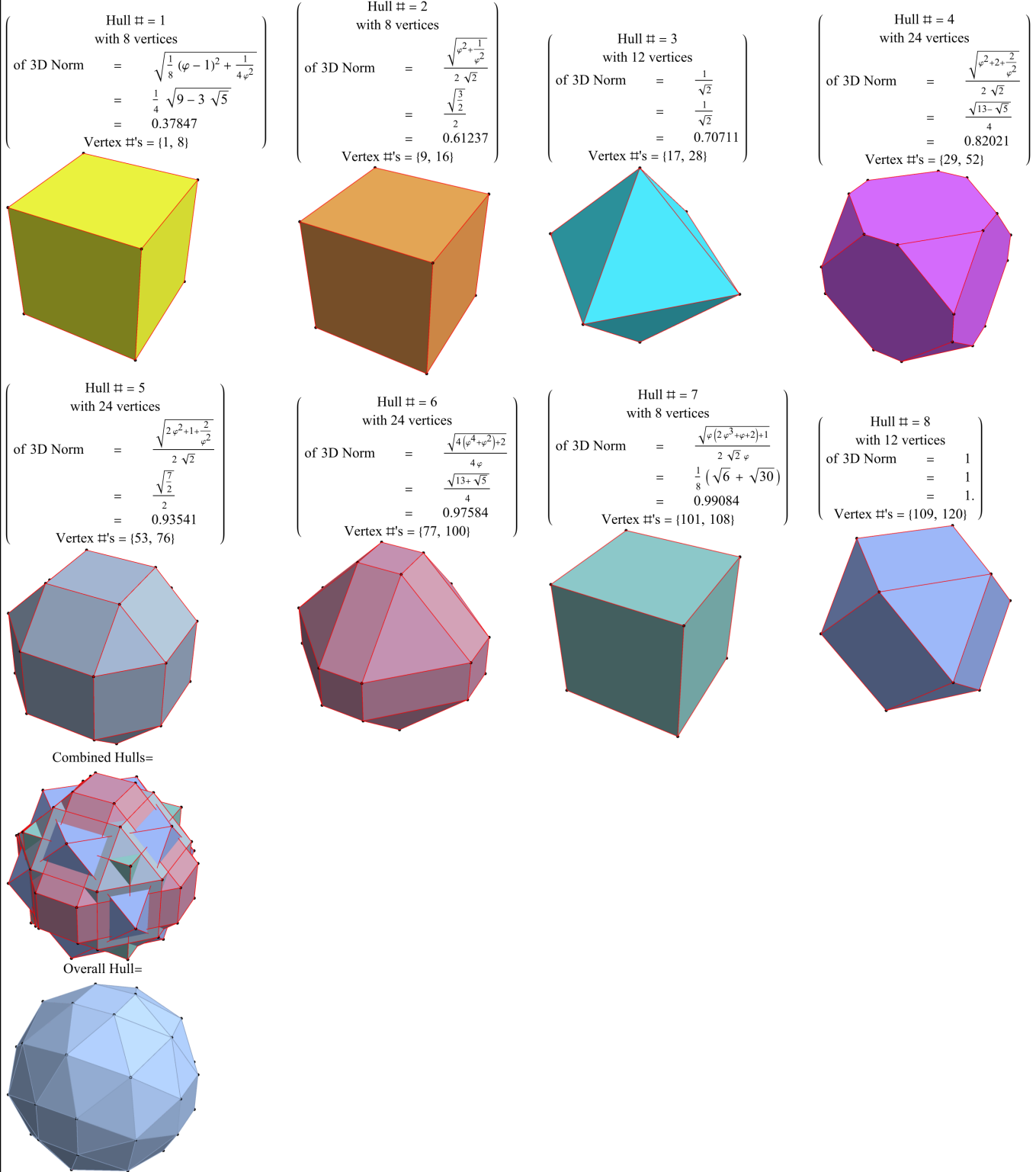


FIG. 15. Concentric hulls of  $I'$  as the parent  $H_4$  600-cell of order 120 in Platonic 3D projection with numeric and symbolic norm distances. This is generated by  $I' = \text{prq}[\alpha^{0-4}, 1, T']$ .

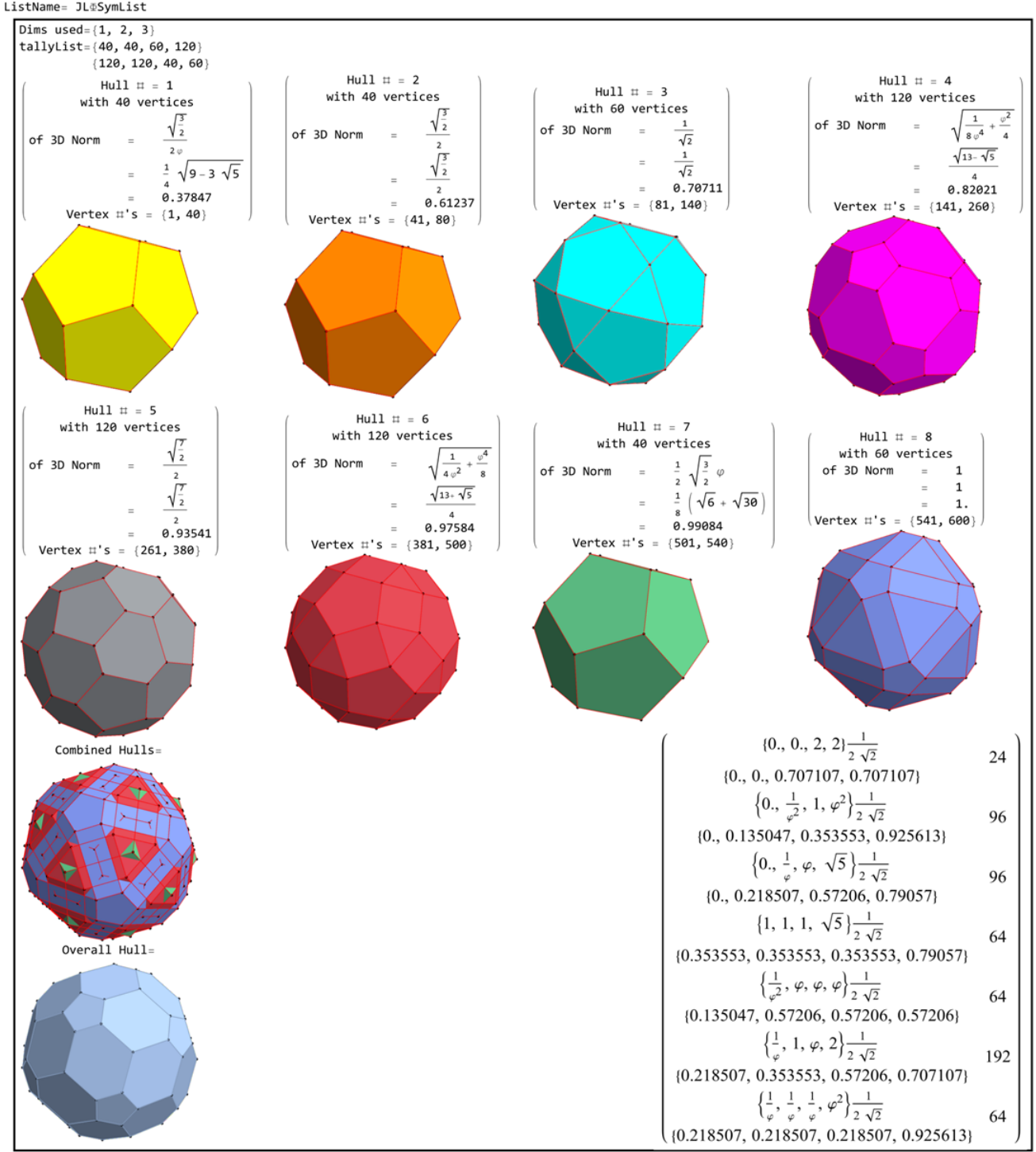


FIG. 16. Concentric hulls of J as the tri-rectified  $H_4$  120-cell of order 600 in Platonic 3D projection with numeric and symbolic norm distances. This is generated by  $J = \text{prq}[A', 1, I] = \text{prq}[A', \alpha^{0-4}, T]$ . Note: The numeric and symbolic tally list of unpermuted vertex values in the lower-right corner

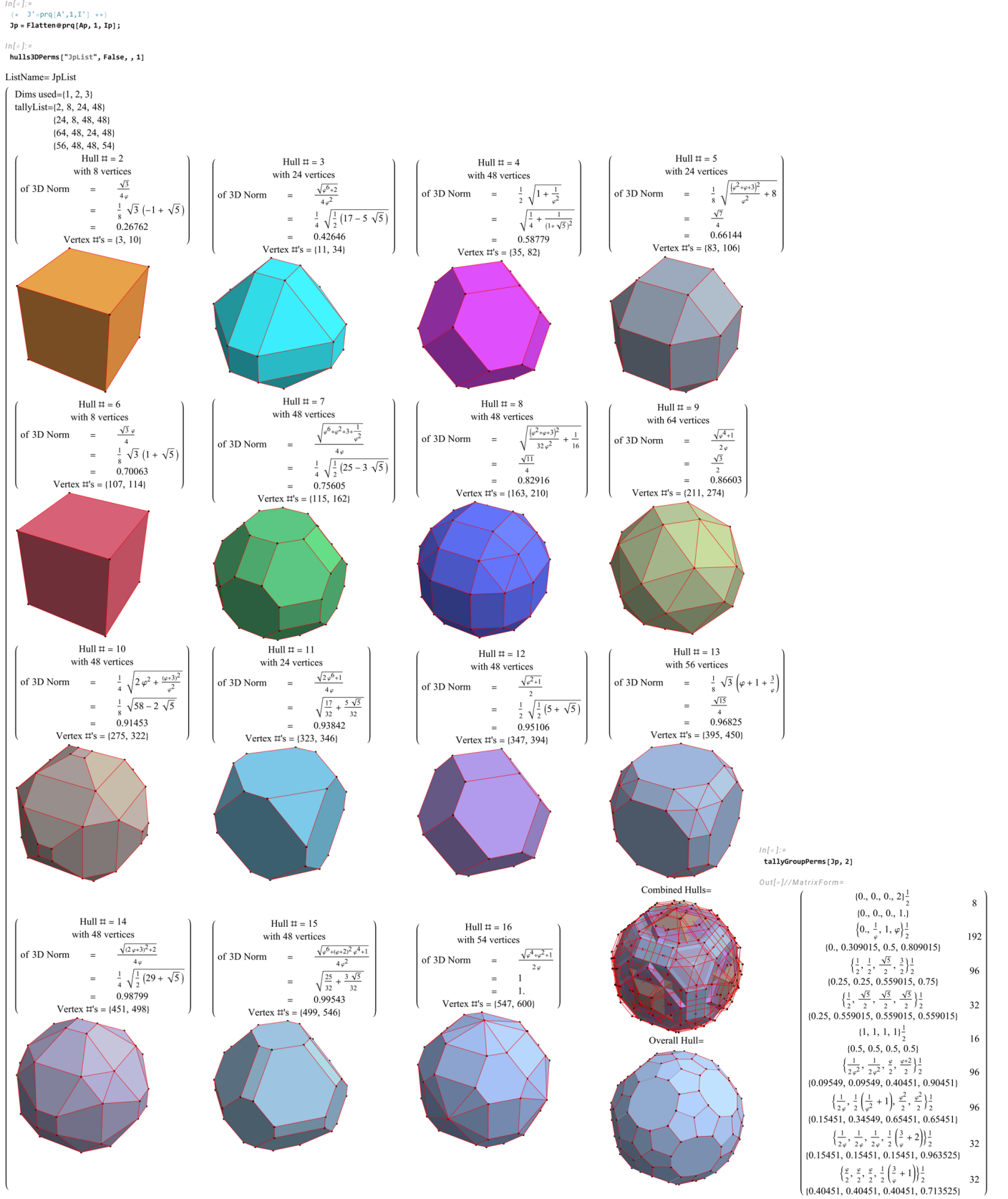


FIG. 17. Concentric hulls of  $J'$  as the tri-rectified  $H_4$  120-cell of order 600 in Platonic 3D projection with numeric and symbolic norm distances. This is generated by  $J' = \text{prq}[A', 1, I'] = \text{prq}[A', \beta^{0-4}, T']$ . Note: The numeric and symbolic tally list of unpermuted vertex values in the lower-right corner



FIG. 18. Archimedean and dual Catalan solids, including their irregular and chiral forms. These were created using quaternion Weyl orbits directly from the  $A_3$ ,  $B_3$ , and  $H_3$  group symmetries[4] listed in the first column.

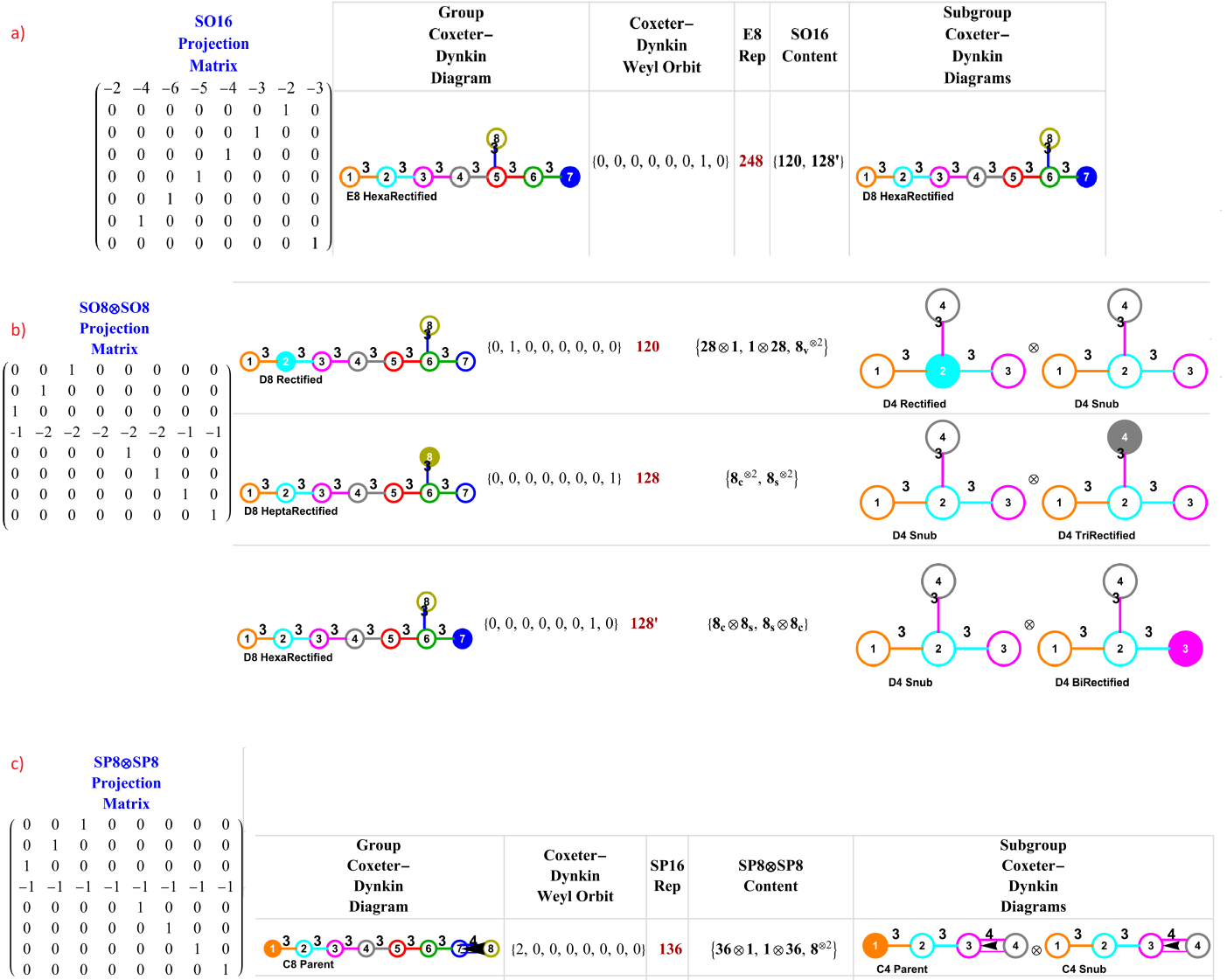


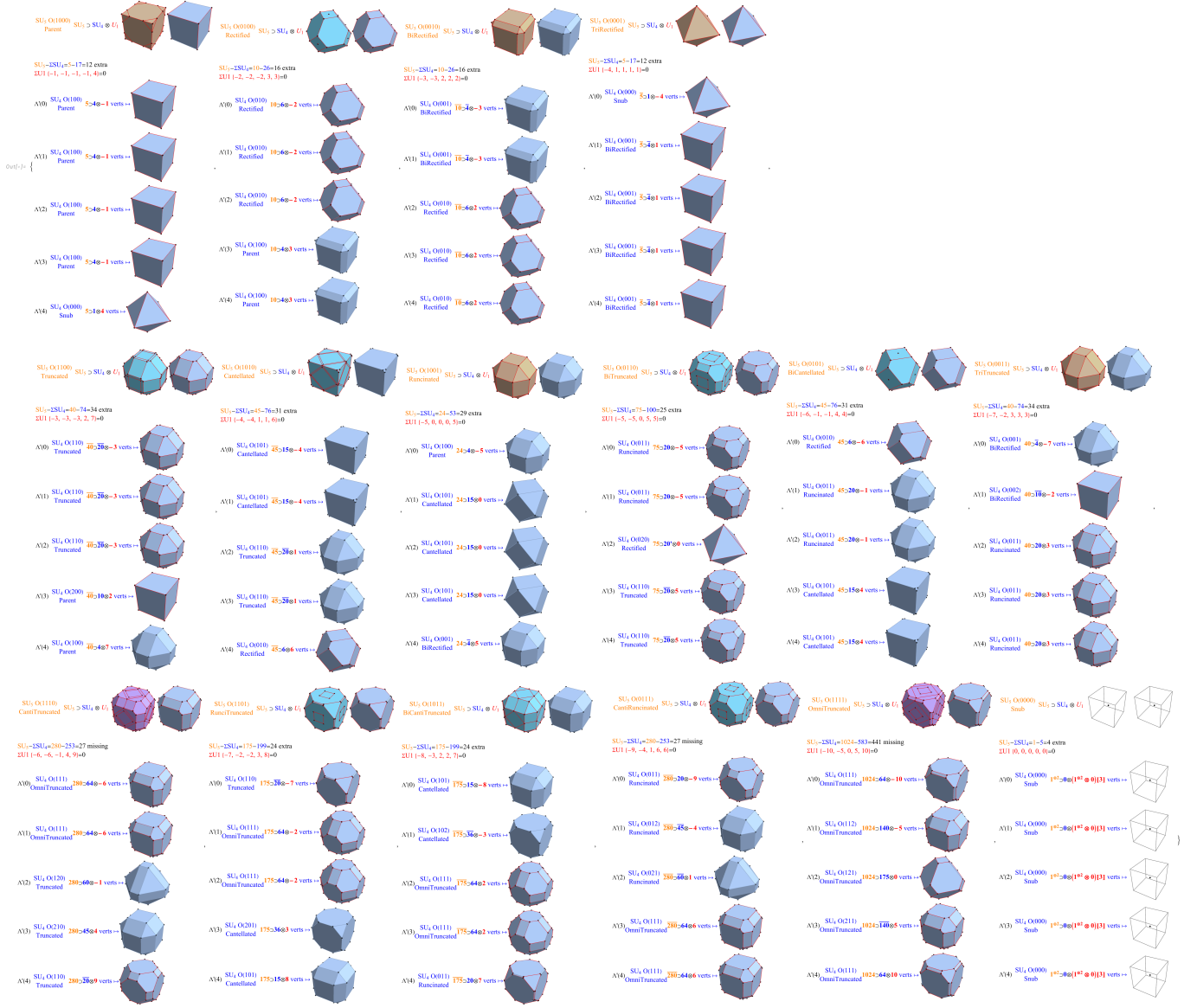
FIG. 19. Breakdown of  $E_8$  maximal embeddings at height 248 of content  $SO(16)=D_8$  (120,128')

a) Height 248  $SO(16)$  content  $120=(112+4+4)+128'$

b) Height 120 and 128'  $SO(8) \otimes SO(8)$  content w/ $8_{v,c,s}^{\otimes 2}$  triality

c) Height 136  $Sp(8) \otimes Sp(8)$  content  $(32+4) \otimes 1, 1 \otimes (32+4), 8^{\otimes 2}$

Note: This output was created in *Mathematica*<sup>TM</sup> with support from the GroupMath[21] and SuperLie[22] packages.





```

(* This switches the H4 (L)eft side scale to the (R)ight side scale (and vice-versa).
We don't use scaleBy if it is a snub 24-cell vertices. *)
switchScale[in_, scaleBy_ : 1] := (* We don't use scaleBy if it is a snub 24-cell vertices. *)
  If[Length@Union@Flatten@Abs@oct2List@N[in /. φRep] == 2,
    in, scaleBy in /. s1Rep];

In[*]:= (* Replacement order is critical *)
mapLRrep = # /. s1Rep & /@ {
  (* φ3 Scale changing: Exchange the ±φ2 ↔ ±1/φ and ±φ3/2 ↔ ±φ3/2 *)
   $\frac{1}{\phi SW^2} \rightarrow \phi, \phi SW^2 \rightarrow \frac{1}{\phi}, \phi SW^{-3/2} \rightarrow \phi^{3/2}, \phi SW^{3/2} \rightarrow \phi^{-3/2},$ 
  (* Sign changing: Exchange the ±√φ ↔ ∓√φ & ±1/√φ ↔ ∓1/√φ, and ±1/φ ↔ ∓1/φ *)
   $\sqrt{\phi SW} \rightarrow -\sqrt{\phi}, \sqrt{\frac{1}{\phi SW}} \rightarrow -\sqrt{\frac{1}{\phi}}, \frac{1}{\phi SW} \rightarrow -\frac{1}{\phi},$ 
  (* Final φ3 Scale changing: ±φ ↔ ±1/φ2 *)
   $\phi SW \rightarrow \frac{1}{\phi^2} (**);$ 
};

In[*]:= (* This processes only individual vertices with a symbolic list input. *)
mapLR[in_, scaleBy_ : 1, uDetIfCorrection_ : True] := Module[{(**)input, output(**)},
  (* Correct for use of √φ in U,
  which produces i values (which may be desired?) *)
  input = If[currU == 11 || ! uDetIfCorrection, in, FullSimplify[in uDetIf /. s1Rep, Assumptions → φAssumptions]];
  output = FullSimplify[switchScale[octSym@input /. φ → φsw /. mapLRrep, scaleBy] ×
    (* Correct back *)
    If[currU == 11 || ! uDetIfCorrection, 1, 1 / uDetIf] /. s1Rep, Assumptions → φAssumptions];
  (* currU < 9 don't reverse the L↔R ordering *)
  If[currU < 9, output, Join[Reverse[output[[ ; 4]], Array[0 &, Length[output] - 4]]]];

(* List and verify the operation of mapLR - one for h48 and one for h4 *)
genE8fromH4@in_String := Module[{indx, inH4 = If[in == "H48", h48, h4], i, j, left, right, h4LR},
  (* Style the Heading in Bold, 24-cell rows in Red, and p48 constraint members marked with an * *)
  Style[#,
    {If[MemberQ[If[in == "H48", h48cell24, h4cell124], indx], Red, Black],
    If[Head@indx === String, Bold, Plain]}] & /@ (indx = #[[2]; #) & /@
  Join[
    (* The Heading row *)
    {{"#", in <> "#", If[labels, "pLb1", Nothing],
      Column[{"E8 vertex", "E8.U=" <> in <> "L" <> "φ" <> in <> "R"}, Center],
      Column[{If[currU == 11, "", "2 "] <> in <> "L", "mapLR("<> in <> "L)=" <> in <> "R"}, Center],
      Column[{If[currU == 11, "", "2 "] <> in <> "R", "mapLR("<> in <> "R)=" <> in <> "L"}, Center],
      Column[{"", "(" <> in <> "L" <> "φ" <> in <> "R" <> ") . U-1=E8 vertex"}, Center],
      Column[{"E8->" <> in <> "L" <> "φ" <> in <> "R" <> "≡", in <> "L" <> "φ" <> in <> "R" <> "→E8"}, Center]}],
    (* Generate data row content *)
    {ToString@# <> If[MemberQ[p48L, #], "*", ""], (* h48[[#]] is an E8 index number to an E8 element in h48 *)
      inH4[[#]], If[labels, plbl@inH4[[#]], Nothing],
      (* Show the E8 vertex *)
      i = pE8@inH4[[#]],
      (* pC600 is converts from E8→H4 using U, here we take the H4 4D left side *)
      If[currU == 11, 1, 2] (left = octSym[pC600[inH4[[#]]][ ; 4]] /. φRuleList),
      (* mapLR converts the H4 4D left side vertex to its corresponding H4 4D right-side vertex,
      which when Joined gives the 8D H4 that can be converted back to E8 by using UInv *)
      If[currU == 11, 1, 2] (right = mapLR@left /. φRuleList),
      (* Conditionally print some cross-checks *)
      print["#=", #, " h4[[#]]=", inH4[[#]], " E8.U=", octSym[pC600[inH4[[#]]] /. φRuleList, " left=", left, " right=", Reverse@right];
      print[" E8.U==Join[left,mapLR@left]=", N@Join[left, right] == N@octSym[pC600[inH4[[#]]] /. φRuleList];
      print[" mapLR@right", If[currU == 11, 1, 2] (mapLR@right /. φRuleList)];
      print[" left==mapLR@right=", N@left == N@mapLR@right /. φRuleList];
      (* Show the H4L↔H4R.UInv vertex *)
      h4LR = Join[left, right];
      j = Rationalize@FullSimplify[Chop[h4LR.UInv /. φRep, chop], Assumptions → φAssumptions],
      (* Check that E8→H4→H4L↔H4R→E8 *)
      j == N@i /. s1Rep & /@ Range@120] // MatrixForm];

```

FIG. 21. *Mathematica*<sup>TM</sup> code to generate the output showing  $E_8 \leftrightarrow H_4$  isomorphism

```
in[]:= curru= 9; setM;
      (octSym#m -> mapLR# / . sRep) &#e { {
        {1 / t, 0, -1, 1 / t^2},
        {-1 / t, 0, 1, -1 / t^2},
        {t, 0, -1, 1 / t},
        {-t, 0, 1, -1 / t} } / If (curru = 11, 1, uDettf) / . sRep // MatrixForm
      )
      (* 24-cell rows in Red and p48 constraint members marked with an * *)
      genE8FromH4#H4"
```

Out[]:= MatrixForm=

#	H4 #	E8 vertex E8U=H4, @H4 #	2 H4 # mapLR(H4)=H4 #	2 H4 # mapLR(H4)=H4 #	(H4 @H4 #)U^1=E8 vertex	E8-H4, @H4 # H4 @H4 # => E8	#	H4 #	E8 vertex E8U=H4, @H4 #	2 H4 # mapLR(H4)=H4 #	2 H4 # mapLR(H4)=H4 #	(H4 @H4 #)U^1=E8 vertex	E8-H4, @H4 # H4 @H4 # => E8
1	13	$(\frac{1}{2}, -\frac{1}{2}, -\frac{1}{2}, -\frac{1}{2}, -\frac{1}{2}, -\frac{1}{2}, -\frac{1}{2}, -\frac{1}{2})$	$(\frac{1}{\sqrt{6}}, -\sqrt{6}, -\frac{1}{\sqrt{6}}, 0)$	$(0, -\varphi^{3/2}, -\sqrt{6}, -\frac{1}{\sqrt{6}})$	$(\frac{1}{2}, -\frac{1}{2}, -\frac{1}{2}, -\frac{1}{2}, -\frac{1}{2}, -\frac{1}{2}, -\frac{1}{2}, -\frac{1}{2})$	True	60	128	$(\frac{1}{2}, -\frac{1}{2}, -\frac{1}{2}, -\frac{1}{2}, -\frac{1}{2}, -\frac{1}{2}, -\frac{1}{2}, -\frac{1}{2})$	$(-\sqrt{6}, -\frac{1}{\sqrt{6}}, 0, -\frac{1}{\sqrt{6}})$	$(\varphi^{3/2}, 0, \frac{1}{\sqrt{6}}, \sqrt{6})$	$(\frac{1}{2}, -\frac{1}{2}, -\frac{1}{2}, -\frac{1}{2}, -\frac{1}{2}, -\frac{1}{2}, -\frac{1}{2}, -\frac{1}{2})$	True

FIG. 22. Output showing detail of  $E_8 \leftrightarrow H_4(L \oplus R \oplus 1 \oplus \varphi)$  isomorphism for each vertex  
 Note: Red rows indicate  $D_4$  24-cell membership and the \* identifies those satisfying the constraint of  $p \in I$  where  $p^5 = \pm 1$ .

